THE EFFECTS OF WAVE ESCAPE ON FAST MAGNETOSONIC WAVE TURBULENCE IN SOLAR FLARES

Peera Pongkitiwanichakul[1], Benjamin D. G. Chandran[1], Judith T. Karpen[2], and C. Richard DeVore[3]

[1] Space Science Center and Department of Physics, University of New Hampshire, Durham, NH 03824, USA; pbu3@unh.edu, benjamin.chandran@unh.edu
[2] NASA Goddard Space Flight Center, Greenbelt, MD 20771, USA; judy.karpen@nasa.gov
[3] Naval Research Laboratory, Washington, DC 20375, USA; devore@nrl.navy.mil

ABSTRACT

One of the leading models for electron acceleration in solar flares is stochastic acceleration by weakly turbulent fast magnetosonic waves ("fast waves"). In this model, large-scale flows triggered by magnetic reconnection excite large-wavelength fast waves, and fast-wave energy then cascades from large wavelengths to small wavelengths. Electron acceleration by large-wavelength fast waves is weak, and so the model relies on the small-wavelength waves produced by the turbulent cascade. In order for the model to work, the energy cascade time for large-wavelength fast waves must be shorter than the time required for the waves to propagate out of the solar-flare acceleration region. To investigate the effects of wave escape, we solve the wave kinetic equation for fast waves in weak turbulence theory, supplemented with a homogeneous wave-loss term. We find that the amplitude of large-wavelength fast waves must exceed a minimum threshold in order for a significant fraction of the wave energy to cascade to small wavelengths before the waves leave the acceleration region. We evaluate this threshold as a function of the dominant wavelength of the fast waves that are initially excited by reconnection outflows.

Key words: plasmas – Sun: corona – Sun: flares – waves

1. INTRODUCTION

Solar flares emit photons across a broad range of wavelengths, with ∼99% of the radiated energy in the optical and UV continuum (Woods et al. 2004; Emslie et al. 2005). Although X-rays and gamma-rays account for only a small fraction of a flare's total radiative luminosity, they provide important diagnostics on the populations of high-energy particles produced by flares. For example, flare X-ray spectra are typically thermal at photon energies $\lesssim 20$ keV and non-thermal (power laws or broken power laws) at energies $\gtrsim 20$ keV (Miller et al. 1997). Most of the X-ray emission is likely bremsstrahlung radiation resulting from Coulomb collisions between thermal protons in the chromosphere and high-energy electrons streaming down from the corona (Aschwanden 2002; Petrosian et al. 2002). Since bremsstrahlung X-ray photons of energy E_1 are typically emitted by proton–electron collisions involving electrons with energies $\sim E_1$, the observed X-ray spectra imply that the electrons typically have thermal distributions at energies $\lesssim 20$ keV and non-thermal distributions at energies $\gtrsim 20$ keV (Miller et al. 1997). The intensity of the X-ray emission can be used to deduce the electron acceleration rate. For example, during the peak of a typical, large X-class flare, the observed X-ray emission implies that electrons are accelerated to energies $\gtrsim 20$ keV at a rate of $\sim 10^{37}$ s^{-1} (Miller et al. 1997).

The origin of these high-energy electrons is a long-standing puzzle. Three main explanations have been advanced in the literature: shock acceleration, acceleration by large-scale, coherent electric fields, and stochastic particle acceleration (SPA; Miller et al. 1997). In this paper, we focus on the SPA model, in which particles are accelerated by electromagnetic fluctuations associated with waves and/or turbulence. In this model, magnetic reconnection in the corona triggers rapid plasma outflows from the reconnection site (Carmichael 1964; Hirayama 1974; Kopp & Holzer 1976; Tsuneta et al. 1992; Tsuneta 1996; Priest & Forbes 2000). Sunward flows encounter closed magnetic loops lower in the solar atmosphere, generating a disordered, turbulent flow above the loop tops. Initially, the

velocity fluctuations in this disordered flow have a correlation length that is some fraction (perhaps ∼1/10) of the loop size ($\sim 10^9$ cm). This length scale is much larger than the proton inertial length $v_A/\Omega_p = 2.3 \times 10^2$ cm $\cdot (n/10^{10}$ cm$^{-3})^{-1/2}$, where $v_A = B_0/\sqrt{4\pi\rho}$ is the Alfvén speed, B_0 is the strength of the background magnetic field, n is the proton number density, ρ is the mass density, and Ω_p is the proton cyclotron frequency. As a consequence, the fluctuations can be approximated as a superposition of magnetohydrodynamic (MHD) waves, i.e., Alfvén waves, fast magnetosonic waves ("fast waves"), and slow magnetosonic waves.

Most SPA models of electron acceleration focus on interactions between electrons and fast waves through a type of resonant wave–particle interaction called transit-time damping (TTD; Miller et al. 1996; Schlickeiser & Miller 1998; Selkowitz & Blackman 2004; Yan & Lazarian 2004; Yan et al. 2008). In TTD, waves and particles satisfy the Landau resonance condition

$$\omega/k_\parallel = v_\parallel, \qquad (1)$$

where ω is the wave frequency, $k_\parallel$ is the component of the wave number $\boldsymbol{k}$ parallel to the mean magnetic field $\boldsymbol{B}_0$, and $v_\parallel$ is the component of the particle velocity along $\boldsymbol{B}_0$. Equation (1) implies that particles "surf" on the wave phase fronts. In TTD, surfing particles are accelerated along $\boldsymbol{B}_0$ by the magnetic-mirror force arising from the perturbations in the magnetic field strength associated with the waves (Stix 1992).

Another ingredient in the electron SPA models cited above is turbulence. After large-scale fast waves are excited by reconnection outflows, the waves interact with one another, causing wave energy to cascade from large wavelengths to smaller wavelengths. This energy cascade plays an important role in SPA models, because the small-wavelength fast waves produced by the turbulent cascade make the largest contribution to the electron acceleration rate via TTD (Miller et al. 1996).

Our principal aim in this paper is to investigate how electron acceleration in SPA models is affected by the escape of fast waves from the flare acceleration region. In low-β

plasmas, where

$$\beta = \frac{8\pi p}{B_0^2} \qquad (2)$$

is the ratio of the thermal pressure p to the magnetic pressure, the fast-wave dispersion relation is

$$\omega = k v_A. \qquad (3)$$

Equation (3) implies that fast waves can propagate at speed v_A in any direction. Fast waves can therefore cross magnetic field lines and leave the acceleration region. If the time required for waves to propagate out of the acceleration region is shorter than the energy cascade time at large wavelengths, then the large-wavelength waves that are excited by reconnection outflows will leave the acceleration region before their energy cascades to small wavelengths, sharply reducing the electron acceleration rate. This point was made previously by Miller et al. (1996). However, these authors did not attempt to calculate the degree to which the electron acceleration rate is reduced by wave escape as a function of flare parameters. In addition, their treatment of the fast-wave cascade was based on an estimate of the energy cascade time that was accurate only to within an unknown factor of order unity. We revisit the effects of wave escape using weak turbulence theory to calculate the energy cascade time from first principles. We describe our model of fast-wave turbulence and wave escape in Section 2, present our numerical results in Section 3, and discuss our conclusions in Section 4.

2. LEAKY-BOX MODEL OF FAST-WAVE TURBULENCE IN FLARES

We employ a "leaky-box" model to describe turbulence and wave escape in flares. We treat the flaring region as a homogeneous plasma with a uniform magnetic field B_0 and define the fast-wave power spectrum $F(k)$, abbreviated F_k, to be twice the fast-wave energy per volume in k-space per unit mass. The total fast-wave energy per unit mass is thus given by

$$U_t = \frac{1}{2} \int F_k \, d^3k. \qquad (4)$$

For simplicity, we assume reflectional symmetry, $F(-k) = F(k)$. We take F_k to evolve in time according to the equation

$$\frac{\partial F_k}{\partial t} = -\frac{F_k}{\tau_{esc}} + \left(\frac{\partial F_k}{\partial t}\right)_{turb} + S_k - \sin^2(\theta)k^8 \nu F_k, \qquad (5)$$

where θ is the angle between k and B_0. The first term on the right-hand side of Equation (5) models wave escape from the flare acceleration region, which is characterized by the timescale

$$\tau_{esc} = \frac{L_f}{v_A}, \qquad (6)$$

where L_f is the size of the flare acceleration region. The term $(\partial F_k/\partial t)_{turb}$ in Equation (5) gives the contribution to $\partial F_k/\partial t$ from wave–wave interactions, discussed below. The next term,

$$S_k = \frac{4\dot{E}_0}{3\pi^{3/2}k_0^3} \left(\frac{k}{k_0}\right)^2 \exp\left(-\frac{k^2}{k_0^2}\right), \qquad (7)$$

is a source term representing fast-wave injection from reconnection outflows. Here, $\dot{E}_0$ is the total wave energy injection rate per unit mass, and k_0 is the wavenumber at which S_k peaks.

The last term on the right-hand side of Equation (5) provides a simple, hyperviscous model for the sink of fast-wave energy at large k resulting from TTD, which transfers energy from fast waves to electrons in flares, as described in the introduction. We have made this term $\propto k^8$ purely for convenience, so that it "turns on" only at the largest wavenumbers in the numerical simulations that we present in the next section. The reason we include a factor of $\sin^2 \theta$ in this term is discussed below.

The form of the term $(\partial F_k/\partial t)_{turb}$ in Equation (5) depends on whether the turbulence is weak or strong. Fast waves at wavevector k are weakly turbulent when

$$\delta v_k \ll v_A, \qquad (8)$$

where δv_k is the rms amplitude of the fast-wave fluctuation velocity at length scale k^{-1} (Kadomtsev 1965). When Equation (8) is satisfied, the linear fast-wave period $P = 2\pi/k v_A^{-1}$ is much shorter than the energy cascade timescale τ_c at wavevector k, and the fluctuations can be described as waves to a good approximation. If Equation (8) is not satisfied, and instead $\delta v_k \gtrsim v_A$, then the turbulence is strong at wavevector k, and $\tau_c \lesssim P$.

Observationally, it is not clear whether solar-flare acceleration regions are in the weak-turbulence or strong-turbulence regimes, and in this paper we do not attempt to resolve the uncertainty in the wave amplitudes in solar flares. Instead, we assume that Equation (8) is at least marginally satisfied at all k (i.e., that $\delta v_k \leqslant 0.3 v_A$ at all k), so that weak-turbulence theory is approximately valid. We focus on this limit because wave escape is most important in this parameter regime. We will not model quantitatively the strong-turbulence case in Section 3. However, our results show that if the wave amplitudes are increased so that they approach the strong-turbulence regime, then the energy cascade proceeds sufficiently rapidly that most of the fast-wave energy dissipates before the waves can escape from the solar-flare acceleration region (see Figure 5).

The wave kinetic equation for weakly turbulent fast waves in low-β plasmas was derived by Chandran (2005, 2008). We set $(\partial F_k/\partial t)_{turb}$ equal to the right-hand side of Equation (6) of Chandran (2005), with the Alfvén-wave power spectrum A_k in that equation set equal to zero:

$$\left(\frac{\partial F_k}{\partial t}\right)_{turb} = \frac{9\pi \sin^2 \theta}{8 v_A} \int d^3p \, d^3q \, [\delta(k - p - q)kq F_p(F_q - F_k)$$
$$+ \, \delta(k + p - q)k(k F_p F_q$$
$$+ \, p F_q F_k - q F_p F_k)] \, \delta(\boldsymbol{k} - \boldsymbol{p} - \boldsymbol{q}). \qquad (9)$$

We have neglected Alfvén waves for simplicity but expect that their inclusion would not significantly alter our conclusions about the effects of wave escape on fast-wave turbulence. Equation (9) is equivalent to the wave kinetic equation for weak acoustic turbulence, up to an overall coefficient (Zakharov & Sagdeev 1970; Zakharov et al. 1992). In both weak fast-wave turbulence and weak acoustic turbulence, waves with collinear wavevectors k, p, and q that satisfy the wavenumber resonance condition $k = p + q$ and frequency matching condition $k = p + q$ interact to produce a weak form of wave steepening, which transfers wave energy from small k to large k along radial lines in k-space. However, fast-wave turbulence differs from acoustic turbulence in the following way. As $\sin \theta$ decreases—i.e., k and B_0 become more closely aligned—fast waves become less compressive, the fast-wave cascade weakens, and the energy cascade time increases. This anisotropy is represented mathematically by the coefficient of $\sin^2 \theta$ in Equation (9). It is
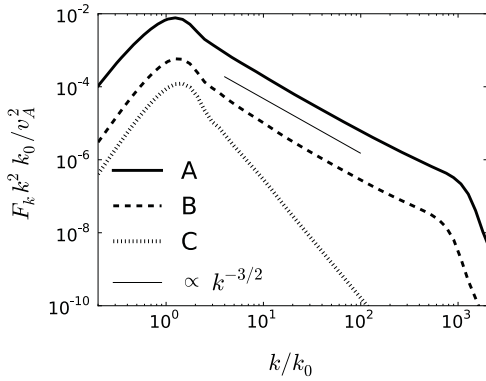
Figure 1. Steady-state fast-wave power spectrum at $\theta = 50°$ in three numerical solutions in which $k_0 L_{\rm f} = 22$. The thin solid line shows the scaling $k^2 F_k \propto k^{-3/2}$ that arises in weak turbulence calculations without wave escape.

Figure 2. Star symbols are the decay timescales T_c computed from numerical integrations of Equation (5) for decaying fast-wave turbulence in the absence of wave escape ($S_k \to 0$ and $\tau_{\rm esc} \to \infty$), and the solid line is an analytic fit to the numerical results, given by Equation (12).

also why we have made the hyperviscosity term in Equation (5) proportional to $\sin^2 \theta$: this dependence prevents the dissipation term from truncating the fast-wave cascade at very small k when $\sin \theta$ is small.

3. NUMERICAL RESULTS

We numerically integrate Equation (5) forward in time until a steady state is reached. To evaluate the nonlinear term $(\partial F_k / \partial t)_{\rm turb}$, we use the energy-conserving numerical algorithm employed by Chandran (2005), which is an extension of the numerical method developed by Leith & Kraichnan (1972) for statistical turbulence theories. We use a logarithmic wavenumber grid in both $k_\perp$ and $k_\parallel$ (the components of $\boldsymbol{k}$ perpendicular and parallel to $\boldsymbol{B}_0$), with $k_{\perp i} = (0.2k_0)2^{i/4}$, $i = 0, 1, 2, \ldots, N-1$, $k_{\parallel 0} = 0$, $k_{\parallel j} = (0.2k_0)2^{(j-1)/4}$, $j = 1, 2, \ldots, N-1$, and $N = 60$. In all of our calculations, we choose the hyperviscosity coefficient ν so that dissipation is negligible at small k ($k \lesssim 10^2$) but strong enough at large k ($k \gtrsim 10^3$) to truncate the cascade.

In Figure 1, we plot three steady-state solutions for F_k at $\theta = 50°$. For each of these solutions, $k_0 L_{\rm f} = 22$. (As shown in the Appendix, the correlation length associated with an isotropic fast-wave spectrum localized at $k = k_0$ is $L_c = 2.2/k_0$; thus, the choice $k_0 L_{\rm f} = 22$ corresponds to $L_c = L_{\rm f}/10$.) For the solutions labeled A, B, and C, $\dot{E}_0$ is chosen so that $U_{\rm t}/U_B$ equals 2.4×10^{-1}, 1.4×10^{-2}, and 2.2×10^{-3}, respectively, where

$$U_B = \frac{v_A^2}{2} \qquad (10)$$

is the energy per unit mass of the background magnetic field. For solution A, F_k possesses a power-law scaling at $k_0 \ll k \ll 10^3 k_0$ in which $k^2 F_k \propto k^{-3/2}$, as in weak fast-wave turbulence in homogeneous plasmas (Cho & Lazarian 2002; Chandran 2005). In solution B, $k^2 F_k$ is slightly steeper than $k^{-3/2}$ at $k \sim 5k_0$ but flattens to become $\propto k^{-3/2}$ at larger k. On the other hand, the fast-wave spectrum is much steeper in solution C than in solutions A and B.[4]

---

[4] We note that if the fast-wave cascade were purely local in k, then F_k would decrease exponentially with increasing k in the escape-dominated case. However, the full weak-turbulence "collision integral" on the right-hand side of Equation (9) includes nonlocal interactions. Thus, the cascade time at large k in the escape-dominated limit becomes independent of k and has a value that is controlled by the amplitude of the power spectrum near k_0. When both the cascade time and the escape time are independent of k, one recovers a power law whose slope depends on the ratio of these two timescales.
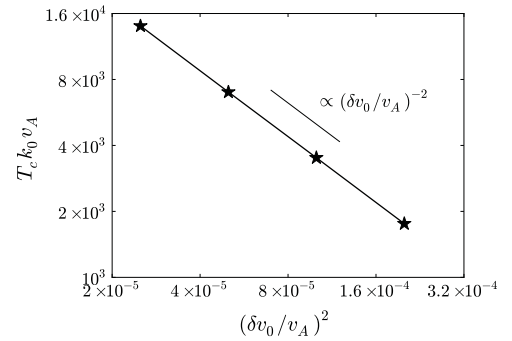
The differing role of wave escape in these three numerical solutions can be understood by comparing the energy cascade time τ_c at $k = k_0$ with the escape time $\tau_{\rm esc}$. The cascade timescale $\tau_c(k)$ can be thought of as the time required for fast-wave energy to cascade from wavenumber k to wavenumber $\sim 3k$. To calculate $\tau_c(k_0)$, we carry out a series of numerical integrations of Equation (5) with $S_k \to 0$ and $\tau_{\rm esc} \to 0$. At $t = 0$, we set

$$F_k = \frac{4U_{\rm t0}}{3\pi^{3/2} k_0^3} \left(\frac{k}{k_0}\right)^2 \exp\left(-\frac{k^2}{k_0^2}\right), \qquad (11)$$

where $U_{\rm t0}$ is a constant that we vary from one numerical calculation to the next. It follows from Equations (4) and (11) that $U_{\rm t0}$ is the fast-wave energy per unit mass at $t = 0$. After integrating Equation (5) forward in time, we record the time T_c at which half of the initial wave energy has been dissipated. The results are shown in Figure 2. The solid line in Figure 2 is a fit to our numerical results, given by

$$T_c = \left[1.4 \, k_0 v_A \left(\frac{U_{\rm t0}}{U_B}\right)\right]^{-1}. \qquad (12)$$

This expression can be compared to the energy cascade timescale in the inertial range of homogeneous, weak, fast-wave turbulence (Chandran 2005),

$$\tau_c(k) \sim \left[\sin^2(\theta) \, k v_A \left(\frac{\delta v_k}{v_A}\right)^2\right]^{-1}, \qquad (13)$$

where

$$\delta v_k = \sqrt{4\pi k^3 F_k} \qquad (14)$$

is approximately the rms amplitude of fast-wave velocity fluctuations at scale $\sim k^{-1}$. The inertial range is the range of wavenumbers $k_0 \ll k \ll k_{\rm d}$, and $k_{\rm d}$ is the wavenumber at which dissipation (in our case hyperviscosity) becomes important. Because most of the wave energy is concentrated near $k = k_0$,

$$U_{\rm t} \sim (\delta v_{k0})^2. \qquad (15)$$

Thus, the value of T_c in Equation (12) is comparable to the value of $\tau_c(k)$ in Equation (13) when k is set equal to k_0, except that the $\sin^2 \theta$ term drops out because T_c is an effective decay timescale integrating over all values of θ.

In weak fast-wave turbulence in the absence of wave escape, $k^2 F_k \propto k^{-3/2}$, $\delta v_k \propto k^{-1/4}$, and $\tau_c(k) \propto k^{-1/2}$ (Cho & Lazarian
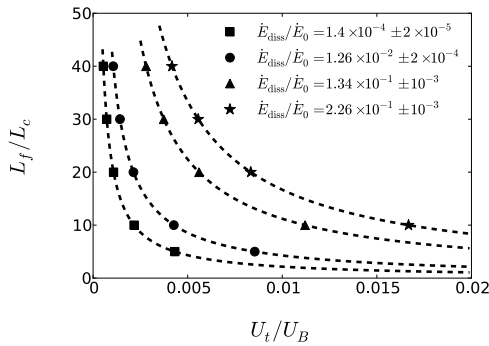
Figure 3. Each symbol corresponds to a numerical solution of Equation (5). The dashed lines correspond to the following values of Γ: 2.16×10^{-2}, 4.26×10^{-2}, 1.12×10^{-1}, and 1.66×10^{-1} (from lower left to upper right). The resulting values of $\dot{E}_{\mathrm{diss}}/\dot{E}_0$ are given in the legend. See the text for details.

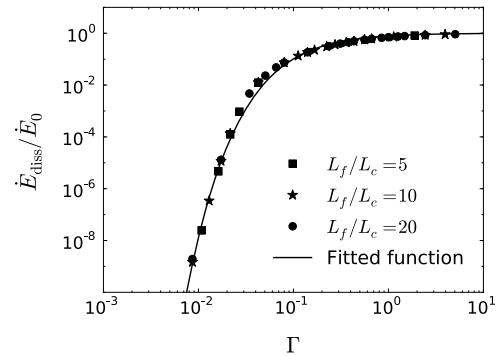**Figure 4.** Each symbol corresponds to a steady-state numerical solution of Equation (5) with one of the three values of $L_{\mathrm{f}}/L_{\mathrm{c}}$ shown in the legend. See the text for details.

2002; Chandran 2005). Because $\tau_{\mathrm{c}}(k) \propto k^{-1/2}$, much of the time T_{c} required for energy to cascade from k_0 to k_{d} is spent cascading from k_0 to $\sim 3k_0$. Thus, the decay timescale T_{c} is comparable to the energy cascade timescale at $k = k_0$; i.e.,

$$\tau_{\mathrm{c}}(k_0) \sim T_{\mathrm{c}}. \qquad (16)$$

On physical grounds, the energy cascade time at $k = k_0$ depends primarily on the values of k_0, U_{t}, and v_{A} (which determine the strength of nonlinear wave–wave interactions at $k = k_0$) and not on whether the turbulence is decaying or forced. We thus take Equation (16) to apply to the forced-turbulence calculations that we present below, but we replace $U_{\mathrm{t}0}$ in Equation (12) with U_{t}, the instantaneous value of the fast-wave energy per unit mass. Equations (12) and (16) then allow us to write

$$\frac{\tau_{\mathrm{esc}}}{\tau_{\mathrm{c}}(k_0)} \sim \Gamma, \qquad (17)$$

where

$$\Gamma \equiv \frac{L_{\mathrm{f}} U_{\mathrm{t}}}{L_{\mathrm{c}} U_B}. \qquad (18)$$

Here, we have re-expressed k_0 in terms of the correlation length of the fast-wave fluctuations, which we take to be (see the Appendix)

$$L_{\mathrm{c}} = \frac{2.2}{k_0}. \qquad (19)$$

We note that the quantities on the right-hand side of Equation (18) are macroscopic parameters that are potentially measurable from observations or MHD simulations of flares.

Returning to the numerical results in Figure 1, when $\tau_{\mathrm{esc}}/\tau_{\mathrm{c}}(k_0)$ is small (as it is for solution C), waves at k_0 escape before their energy cascades to larger k. This causes F_k to steepen and reduces the fraction of the fast-wave energy that is dissipated at large k (i.e., transferred to electrons via TTD in a flare). On the other hand, when the ratio in Equation (17) is $\gtrsim 1$ (as it is for Solution A), fast-wave energy cascades from k_0 to larger wavenumbers before the waves escape, and F_k approaches the scaling found in homogeneous turbulence simulations without wave escape.

In Figure 3, we summarize results from 18 different numerical solutions to Equation (5). To obtain these solutions, we start by fixing the value of $L_{\mathrm{f}}/L_{\mathrm{c}}$ at 5, 10, 20, 30, or 40. We then vary $\dot{E}_0$ until Γ has one of four values: 2.16×10^{-2}, 4.26×10^{-2}, 1.12×10^{-1}, or 1.66×10^{-1}. In the figure, we plot one symbol for each of the solutions, with a different symbol for each of the

four values of Γ. After each solution reaches steady state, we calculate the dissipation power

$$\dot{E}_{\mathrm{diss}} = \int \sin^2(\theta) k^8 \nu F_k \, d^3k \qquad (20)$$

in that solution. Since the dissipation in our simulation is a proxy for the transfer of large-k wave energy to electrons via TTD, the ratio $\dot{E}_{\mathrm{diss}}/\dot{E}_0$ is a measure of the efficiency of electron acceleration. As shown in the legend, the value of this ratio is roughly the same for all simulations with the same value of Γ, i.e., along each of the four curves. This demonstrates that $\dot{E}_{\mathrm{diss}}/\dot{E}_0$ depends almost solely on Γ, i.e., on $\tau_{\mathrm{esc}}/\tau_{\mathrm{c}}(k_0)$.

In Figure 4, we plot $\dot{E}_{\mathrm{diss}}/\dot{E}_0$ for values of Γ ranging from 8.6×10^{-3} to 5.0. For these calculations, we employed three different values for the quantity $L_{\mathrm{f}}/L_{\mathrm{c}}$: 5, 10, and 20. As the figure shows, all three sets of calculations produce essentially the same plot, again supporting our assertion that $\dot{E}_{\mathrm{diss}}/\dot{E}_0$ in our model is determined almost exclusively by the single quantity Γ. The solid line in this plot corresponds to the function

$$\frac{\dot{E}_{\mathrm{diss}}}{\dot{E}_0} = \left(1 + \frac{0.012}{\Gamma}\right)^{-20 + 0.02\Gamma^{-1}} \qquad (21)$$

and provides a reasonable fit to our numerical results.

For fast waves propagating in low-β plasmas, half of the wave energy is in the velocity fluctuations and half is in the magnetic-field fluctuations. The total fast-wave energy is thus twice the energy in the fluctuating magnetic field. If δB is defined to be the rms amplitude of the magnetic-field fluctuations, then $U_{\mathrm{t}}/U_B = 2(\delta B/B_0)^2$. We can thus rewrite Equation (18) as

$$\Gamma = 2\left(\frac{L_{\mathrm{f}}}{L_{\mathrm{c}}}\right)\left(\frac{\delta B}{B_0}\right)^2. \qquad (22)$$

In Figure 5, we use Equations (21) and (22) to plot $\dot{E}_{\mathrm{diss}}/\dot{E}_0$ as a function of $\delta B/B_0$ for three choices of the ratio $L_{\mathrm{f}}/L_{\mathrm{c}}$. The results show that the rate of energy dissipation (i.e., of energy transfer to electrons via TTD) falls off rapidly below rms fast-wave amplitudes $\delta B/B_0$ of about 5%–10%, depending on the size of the flare region relative to the correlation length (outer scale) of the turbulence. In the strong-turbulence limit of larger fast-wave amplitudes, on the other hand, the energy dissipated at shorter wavelengths (transferred to electrons via TTD) approaches 100% of the input wave energy.
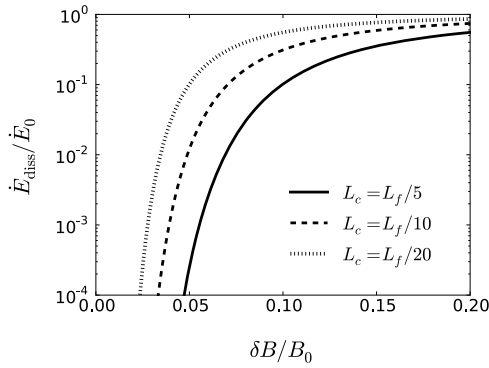
Figure 5. Each of the three curves is a plot of Equation (21) for a different choice of L_f/L_c. See the text for details.

4. CONCLUSION

We have developed a leaky-box model for fast-wave turbulence in solar flares that accounts for wave escape from the solar-flare acceleration region in an approximate way. In this model, we determine the fast-wave power spectrum F_k by solving the wave kinetic equation for fast waves from weak turbulence theory (Chandran 2005, 2008) after modifying this equation in the following ways. First, we set the amplitudes of the other wave types (the slow magnetosonic wave and Alfvén wave) to zero, thereby neglecting interactions between fast waves and other wave types. Second, we add a homogeneous loss term to account for wave escape. Third, we add a source term $S(\boldsymbol{k})$ to model the generation of fast waves by the disordered flows that are presumed to arise when reconnection outflows encounter closed magnetic loops lower in the solar atmosphere. This source term is isotropic in wavenumber space, peaks at a wavenumber k_0, and injects fast-wave energy per unit mass at the rate $\dot{E}_0$, which is an adjustable parameter. Fourth, we add a hyperviscous dissipation term, so that virtually all the energy that cascades to large k is dissipated. The energy dissipation rate per unit mass $\dot{E}_{\rm diss}$ is a proxy for the power (per unit mass) that is available to accelerate particles through wave–particle interactions at large wavenumbers.

We numerically integrate this modified wave kinetic equation forward in time until a steady state is reached, varying $\dot{E}_0$ and the quantity $k_0 L_f$, where L_f is the size of the flare acceleration region. We find that the acceleration efficiency, $\dot{E}_{\rm diss}/\dot{E}_0$, depends on a single quantity, Γ (defined in Equation (18)), which is approximately the ratio of the escape time $\tau_{\rm esc}$ to the energy cascade time at k_0, which is denoted $\tau_c(k_0)$. When $\tau_{\rm esc} \ll \tau_c(k_0)$, almost all of the fast-wave power that is injected at wavenumber k_0 escapes the flare acceleration region before cascading to small scales. On the other hand, if $\tau_{\rm esc} \gtrsim \tau_c(k_0)$, then a sizable fraction of the fast-wave power that is injected at k_0 cascades to large k and dissipates before leaving the flare acceleration region.

To gain further insight into the effects of wave escape on electron acceleration by fast waves in solar flares, it will be important to obtain stronger constraints on U_t/U_B and L_f/L_c in flares. One way that such constraints could be obtained is through numerical simulations of magnetic reconnection, outflows, and large-scale magnetic structure in solar flares.

APPENDIX

RELATION BETWEEN WAVENUMBER AND CORRELATION LENGTH

We consider a superposition of waves, all with the same wavenumber k, but with a distribution of wavevector directions that becomes isotropic in the limit that the number of waves is increased toward infinity. We take the phase of each wave to have a random additive phase constant that is uniformly distributed between 0 and 2π. If $f(x)$ is some quantity that is modulated by waves—e.g., a component of the magnetic field—then we can write

$$f(\boldsymbol{x}) = \sum_{i=0}^{N} \sum_{j=1}^{2N} A(\boldsymbol{k}_{ij}) \sin(\boldsymbol{k}_{ij} \cdot \boldsymbol{x} + \psi_{ij}), \qquad (\text{A1})$$

where $\boldsymbol{k}_{ij} = k[(1 - \mu_i^2)^{1/2} \cos \phi_j \hat{x} + (1 - \mu_i^2)^{1/2} \sin \phi_j \hat{y} + \mu_i \hat{z}]$, $\mu_i = 2i/N - 1$, $\phi_j = 2\pi j/N$, and ψ_{ij} is the random, additive phase constant. We set

$$A(\boldsymbol{k}_{ij}) = A_N, \qquad (\text{A2})$$

where A_N is independent of $\boldsymbol{k}_{ij}$ but decreases as N increases so that $\langle |f(x)|^2 \rangle$ remains finite as $N \to \infty$. Because A_N is independent of $\boldsymbol{k}_{ij}$, the power spectrum of f becomes isotropic as $N \to \infty$.

The autocorrelation function of $f(x)$ is

$$C(\boldsymbol{x}) = \frac{\langle f(\boldsymbol{x}_0) f(\boldsymbol{x}_0 + \boldsymbol{x}) \rangle}{\langle f(\boldsymbol{x}_0) f(\boldsymbol{x}_0) \rangle}, \qquad (\text{A3})$$

where $\langle \ldots \rangle$ denotes an ensemble average—i.e., an average over the random phases of the waves. Making use of the relations

$$\langle \sin(\psi_{ij}) \sin(\psi_{mn}) \rangle = \langle \cos(\psi_{ij}) \cos(\psi_{mn}) \rangle = \frac{\delta_{im} \delta_{jn}}{2} \qquad (\text{A4})$$

and

$$\langle \sin(\psi_{ij}) \cos(\psi_{mn}) \rangle = 0, \qquad (\text{A5})$$

we find that

$$\langle f(\boldsymbol{x}_0) f(\boldsymbol{x}_0 + \boldsymbol{x}) \rangle = \frac{A_N^2}{2} \sum_{i=0}^{N} \sum_{j=1}^{2N} \cos(\boldsymbol{k}_{ij} \cdot \boldsymbol{x}) \qquad (\text{A6})$$

and

$$\langle f(\boldsymbol{x}_0) f(\boldsymbol{x}_0) \rangle = \chi, \qquad (\text{A7})$$

where

$$\chi = \lim_{N \to \infty} N(N + 1) A_N^2. \qquad (\text{A8})$$

In the limit $N \to \infty$, $C(\boldsymbol{x})$ depends only on $|\boldsymbol{x}|$. We thus define

$$C(x) = \lim_{N \to \infty} C(\boldsymbol{x}). \qquad (\text{A9})$$

Without loss of generality, we set $\boldsymbol{x} = x\hat{z}$ to obtain

$$\lim_{N \to \infty} \langle f(\boldsymbol{x}_0) f(\boldsymbol{x}_0 + \boldsymbol{x}) \rangle = \frac{\chi}{2} \int_{-1}^{1} d\mu \cos(\mu k x) = \frac{\chi \sin(kx)}{kx}. \qquad (\text{A10})$$

Equations (A7) and (A10) imply that

$$C(x) = \frac{\sin(kx)}{kx}. \tag{A11}$$

We define the correlation length of $f(x)$, L_c, through the relation

$$C(L_c) = e^{-1}. \tag{A12}$$

This gives

$$L_c = \frac{2.2}{k}. \tag{A13}$$

REFERENCES

Aschwanden, M. J. 2002, Space Sci. Rev., 101, 1
Carmichael, H. 1964, in NASA Special Publication, Vol. 50, The Physics of Solar Flares, ed. W. N. Hess (Washington, DC: NASA), 451
Chandran, B. D. G. 2005, Phys. Rev. Lett., 95, 265004
Chandran, B. D. G. 2008, Phys. Rev. Lett., 101, 235004
Cho, J., & Lazarian, A. 2002, Phys. Rev. Lett., 88, 245001
Emslie, A. G., Dennis, B. R., Holman, G. D., & Hudson, H. S. 2005, J. Geophys. Res., 110, A11103
Hirayama, T. 1974, Sol. Phys., 34, 323
Kadomtsev, B. B. 1965, Plasma Turbulence (London: Academic)
Kopp, R. A., & Holzer, T. E. 1976, Sol. Phys., 49, 43
Leith, C. E., & Kraichnan, R. H. 1972, J. Atmos. Sci., 29, 1041
Miller, J. A., Cargill, P. J., Emslie, A. G., et al. 1997, J. Geophys. Res., 102, 14631
Miller, J. A., LaRosa, T. N., & Moore, R. L. 1996, ApJ, 461, 445
Petrosian, V., Donaghy, T. Q., & McTiernan, J. M. 2002, ApJ, 569, 459
Priest, E., & Forbes, T. 2000, Magnetic Reconnection (Cambridge: Cambridge Univ. Press)
Schlickeiser, R., & Miller, J. A. 1998, ApJ, 492, 352
Selkowitz, R., & Blackman, E. G. 2004, MNRAS, 354, 870
Stix, T. H. 1992, Waves in Plasmas (New York: Springer)
Tsuneta, S. 1996, ApJ, 456, 840
Tsuneta, S., Hara, H., Shimizu, T., et al. 1992, PASJ, 44, L63
Woods, T. N., et al. 2004, Geophys. Res. Lett., 311, L10802
Yan, H., & Lazarian, A. 2004, ApJ, 614, 757
Yan, H., Lazarian, A., & Petrosian, V. 2008, ApJ, 684, 1461
Zakharov, V. E., L'vov, V. S., & Falkovich, G. 1992, Kolmogorov Spectra of Turbulence I (Berlin: Springer)
Zakharov, V. E., & Sagdeev, R. Z. 1970, Sov. Phys. Dokl., 15, 439